

## Contrast of Rainfall–SST Relationships in the Western North Pacific between the ENSO-Developing and ENSO-Decaying Summers\*

BO WU

*LASG, Institute of Atmospheric Physics, Chinese Academy of Sciences, and Graduate University of Chinese Academy of Sciences, Beijing, China*

TIANJUN ZHOU

*LASG, Institute of Atmospheric Physics, Chinese Academy of Sciences, Beijing, China*

TIM LI

*IPRC, and Department of Meteorology, University of Hawaii at Manoa, Honolulu, Hawaii*

(Manuscript received 30 May 2008, in final form 5 February 2009)

### ABSTRACT

While the overall summer rainfall–sea surface temperature (SST) relationship has a negative correlation over the western North Pacific (WNP), this relationship experiences a significant interannual variation. During the ENSO-developing (decaying) summer, the rainfall–SST correlation is significantly positive (negative). The positive correlation is attributed to interplay between the anomalous Walker circulation and the cross-equatorial flows associated with the enhanced WNP summer monsoon. The former leads to negative rainfall anomalies in the western Pacific, whereas the latter leads to a cold SST anomaly resulting from enhanced surface latent heat fluxes. The negative correlation is attributed to the maintenance of an anomalous Philippine Sea anticyclone from the El Niño peak winter to the subsequent summer. The anomalous anticyclone, on one hand, suppresses the local rainfall, and on the other hand induces a warm in situ SST anomaly through both the enhanced solar radiation (resulting from a decrease in clouds) and the reduced surface latent heat flux (resulting from the decrease of the monsoon westerly). The rainfall–SST correlation is insignificant in the remaining summers. Thus, the overall weak negative rainfall–SST correlation is attributed to the significant negative correlation during the ENSO-decaying summers.

### 1. Introduction

Previous studies revealed a negative correlation between rainfall and underlying sea surface temperature (SST) anomalies (SSTAs) over the western North Pacific (WNP) in boreal summer (Trenberth and Shea 2005; Wang et al. 2005). The maximum rainfall phase leads that of the cold SSTA by 1 month, suggesting that the ocean,

to the first order of approximation, is a passive response to the in situ atmospheric forcing (Wang et al. 2005). Atmospheric general circulation models (AGCMs) generally have less skills in simulating the WNP summer monsoon because of the lack of air–sea coupling (Wang et al. 2004, 2005; Wu et al. 2006; Zhou et al. 2008a,b, 2009). The negative SST tendency–rainfall correlation poses a challenge to the current two-tier strategy for seasonal climate forecast. It implies that atmospheric forcing may play a dominant role in the WNP summer monsoon region (Wu et al. 2006; Wu and Kirtman 2007).

The WNP summer monsoon exhibits a pronounced quasi-biennial variability and is a key region for generating the troposphere biennial oscillation in the warm pool (Li et al. 2006). In association with remote El Niño forcing, a phase-dependent low-frequency atmospheric circulation controls the WNP, with a pronounced anomalous

---

\* School of Ocean and Earth Science and Technology Contribution Number 7667 and International Pacific Research Center Contribution Number 600.

---

Corresponding author address: Dr. Tianjun Zhou, LASG, Institute of Atmospheric Physics, Chinese Academy of Sciences, Beijing 100029, China.  
E-mail: zhoutj@lasg.iap.ac.cn

TABLE 1. Classification of the 1979–2005 summers into DV, DC, and RM summers.

Type	El Niño	La Niña
DV	1982, 1987, 1991, 1994, 1997, 2002, 2004	1999
DC	1983, 1988, 1992, 1995, 1998, 2003, 2005	1984, 1985, 1989, 1996, 2000, 2001
RM	1979, 1980, 1981, 1986, 1990, 1993	

cyclone (anticyclone) during its developing (decaying) summers (Wang et al. 2003). While the anomalous cyclone is a direct Rossby wave response to the central Pacific heating in the El Niño developing phase, the maintenance of the anomalous anticyclone from the northern winter to the subsequent summer is primarily attributed to a positive local thermodynamic air–sea feedback mechanism (Wang et al. 2000). The strongly asymmetric circulation features associated with the ENSO turnabout were also found in other previous studies (Kumar and Hoerling 2003).

Given the distinctive summer circulation patterns between the El Niño–developing and El Niño–decaying phases, some key scientific questions related to the local rainfall–SST relationship need to be investigated. For example, is there an asymmetry regarding the rainfall–SST relationship between the developing and decaying phases of ENSO? If a phase-dependent asymmetric relationship does exist, what are the physical and dynamical processes that are responsible for this asymmetry? In this note, we will explore the asymmetric features of and physical mechanisms for the ENSO phase-dependent rainfall–SST relationships over the WNP.

The rest of this work is organized as follows. After a description of the datasets in section 2, we classify the summer seasons of 1979–2005 into three types based on the ENSO phases and analyze different rainfall–SST relationships for each type in section 3. A summary and discussion are presented in section 4.

## 2. Datasets and methods

The data used in the present study consist of 1) the Met Office’s Hadley Center’s Sea Ice and SST dataset version 1 (HadISST1) from 1979 to 2005 (Rayner et al. 2003), 2) precipitation data of the Climate Prediction Center (CPC) Merged Analysis of Precipitation (CMAP) from 1979 to 2005 (Xie and Arkin 1997), 3) precipitation data of the Global Precipitation Climatology Project (GPCP) from 1979 to 2005 (Adler et al. 2003), 4) the National Center for Environment Prediction–National Center for Atmospheric Research (NCEP–NCAR) reanalysis data from 1979 to 2005 (Kalnay et al. 1996), 5)

objectively analyzed air–sea fluxes for global oceans (OAFlux) from 1984 to 2002 (Yu et al. 2008), and 6) Extended Reconstructed Sea Surface Temperature (ERSST), version 3, from 1979 to 2005 (Smith et al. 2008).

In addition, we use the ENSO index derived from the CPC in National Oceanic and Atmospheric Administration (NOAA; information available online at [http://www.cpc.ncep.noaa.gov/products/analysis\\_monitoring/ensostuff/ensoyears.shtml](http://www.cpc.ncep.noaa.gov/products/analysis_monitoring/ensostuff/ensoyears.shtml)). Warm and cold episodes are determined based on a threshold of  $\pm 0.5^{\circ}\text{C}$  for the 3-month running mean of ERSST version 2 SST anomalies in the Niño-3.4 region ( $5^{\circ}\text{N}$ – $5^{\circ}\text{S}$ ,  $120^{\circ}$ – $170^{\circ}\text{W}$ ), and based on the 1971–2000 period.

Based on the Niño-3.4 index, we classify the entire 27 summers from 1979 to 2005 into ENSO-developing (DV) and ENSO-decaying (DC) summers and remaining (RM) summers (see Table 1). Out of the 27 summers, 21 are associated with ENSO. Further, 10 summers satisfy the following two criteria: the absolute value of the June–August (JJA) Niño-3.4 index is larger than  $0.5^{\circ}\text{C}$ ; ENSO reaches a mature phase in the following winter. Eight out of the 10 summers are classified as being the DV type, with the exception of 1983 and 1998. Fifteen summers satisfy the criterion of following an ENSO mature winter. Thirteen out of the 15 summers are classified as being the DC type, with the exception of 1987 and 1999. The remaining six summers not associated with ENSO are classified as being the RM type.

Because of the complexity of ENSO evolution, some exceptions exist in the classification. There are some special occasions. 1) In the 1983 and 1998 summers, while a strong El Niño event dies out, a La Niña event occurs. 2) Because 1986 and 1998 events last longer than 1 yr, 1987 and 1999 summers not only follow but also precede an ENSO mature winter. We classify the 1983 and 1998 events as DC types and the 1987 and 1999 events as DV types, because their circulation and precipitation anomalies in the WNP are close to other DC or DV summers.

Correlation and composite analyses are used to investigate the relationship between precipitation and SST in the WNP in different types. In the DV type, the amount of El Niño events is far more than that of La Niña events (seven versus one), because most La Niña events begin after the summer period. To avoid excessively magnifying the weight of La Niña events, we do not apply the common El Niño composite minus the La Niña composite to the DV type. The only a La Niña event is reversed to an El Niño event through multiplying by  $-1$ . The El Niño composite is performed to represent the features of DV summer. In the DC type, the sample sizes of El Niño and La Niña are comparable. Thus, composites are performed using the El Niño composite

minus the La Niña composite. In addition, a partial correlation is also used in the analysis.

All of the statistically significant tests for correlations and composites are performed using a two-tailed Student's  $t$  test. The degree of freedom is calculated by subtracting the total sample size minus 2, except for the composite analysis for the DV type. A paired difference test is performed for the summer type. Therefore, the degree of freedom is the sample size minus 1. In addition to the local significance test, a more stringent field significant test for the composite is performed using Monte Carlo simulation (Livezey and Chen 1983). The test takes into account the effects of number and interdependence in evaluating the collective significance of finite dataset.

### 3. Results

The spatial distribution of rainfall–SST correlation coefficients for all of the summer (JJA) of 1979–2005 is shown in Fig. 1a. The rainfall data and SST data are derived from the CMAP and HadISST datasets, respectively. The sample number for all years, DV, DC, and RM are 27, 8, 13, and 6, respectively. Their statistical significances at 5% level are 0.38, 0.71, 0.55 and 0.81, respectively. Consistent with the previous studies (Wang et al. 2005), SST is negatively correlated with rainfall over the WNP for the entire 27-yr period, but the correlation hardly exceeds the 5% significance level, except only over a small portion of the WNP. By separating all of the summers into the DV, DC, and RM summers (see Table 1), one may examine the SST–rainfall relationship for each group. It is noted that the rainfall is positively correlated with SSTA over the WNP for the DV type. On the contrary, the SST–rainfall correlation for the DC type is negative over this region (Fig. 1c). The correlation pattern for the DC type generally resembles that for all of the summer, implying that the overall negative SST–rainfall correlation in the region is mainly contributed by the DC type. Compared with the DC and DV types, the RM type has no consistently positive or negative rainfall–SST correlation in the region.

To more clearly illustrate the distinctive rainfall–SST relationships, we plot the scatter diagrams of the box-averaged ( $2.5^{\circ}$ – $15^{\circ}$ N,  $120^{\circ}$ – $140^{\circ}$ E) SST and rainfall anomalies in Fig. 2. To expand the sample size and deduce the data dependence, the GPCP precipitation data and ERSST data are also included in the figure, in addition to the CMAP precipitation data and HadISST data. The sample sizes increase twice. The statistical significances at the 5% level for 54, 16, 26, and 12 sample sizes are 0.27, 0.50, 0.38, and 0.58, respectively. Consistent with Fig. 1a, the area-averaged SST–rainfall correlation for

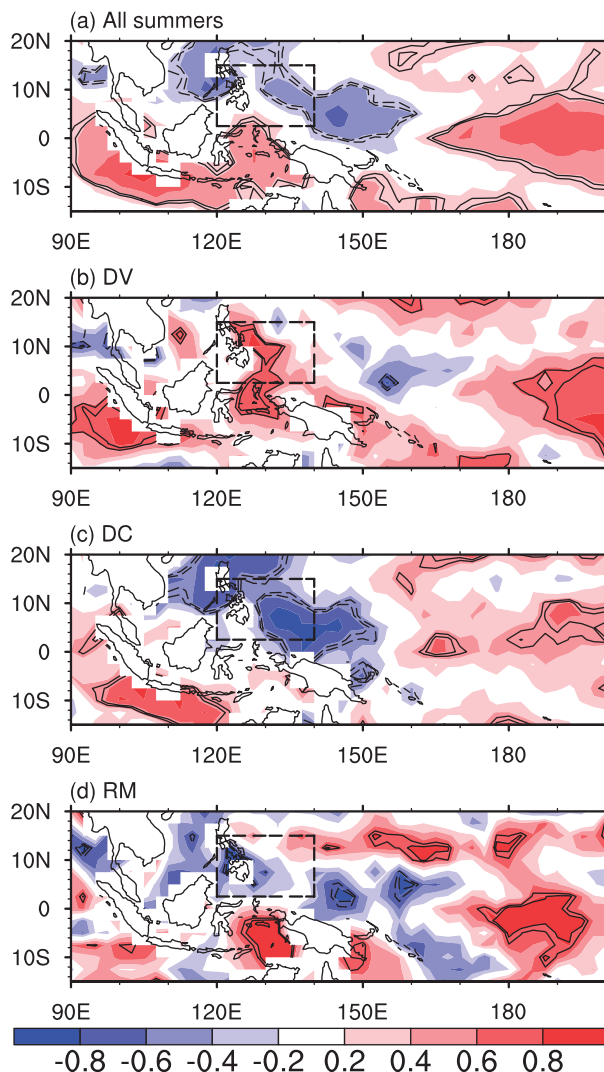


FIG. 1. Patterns of correlation coefficients between the JJA SST and precipitation anomalies for (a) all summers of 1979–2005, (b) ENSO-developing summers, (c) ENSO-decaying summers, and (d) remaining summers. The precipitation and SST are derived from CMAP and HadISST, respectively. Contour lines represent the 5% and 10% significance levels.

all of the summers is only  $-0.26$ , which hardly reaches the 5% significance level (Fig. 2a). By separating ENSO-developing and ENSO-decaying summers, we note that the rainfall is positively correlated with SSTA over the region for the DV type (Fig. 2b), with a positive correlation coefficient of 0.79, exceeding the 5% significance level. On the contrary, the averaged SST–rainfall correlation for the DC type is significantly negative (Fig. 2c), with a correlation coefficient of  $-0.64$ , which also exceeds the 5% significance level. Different from the DC and DV types, the RM type shows no significant SST–rainfall correlation in the region (Fig. 2d).

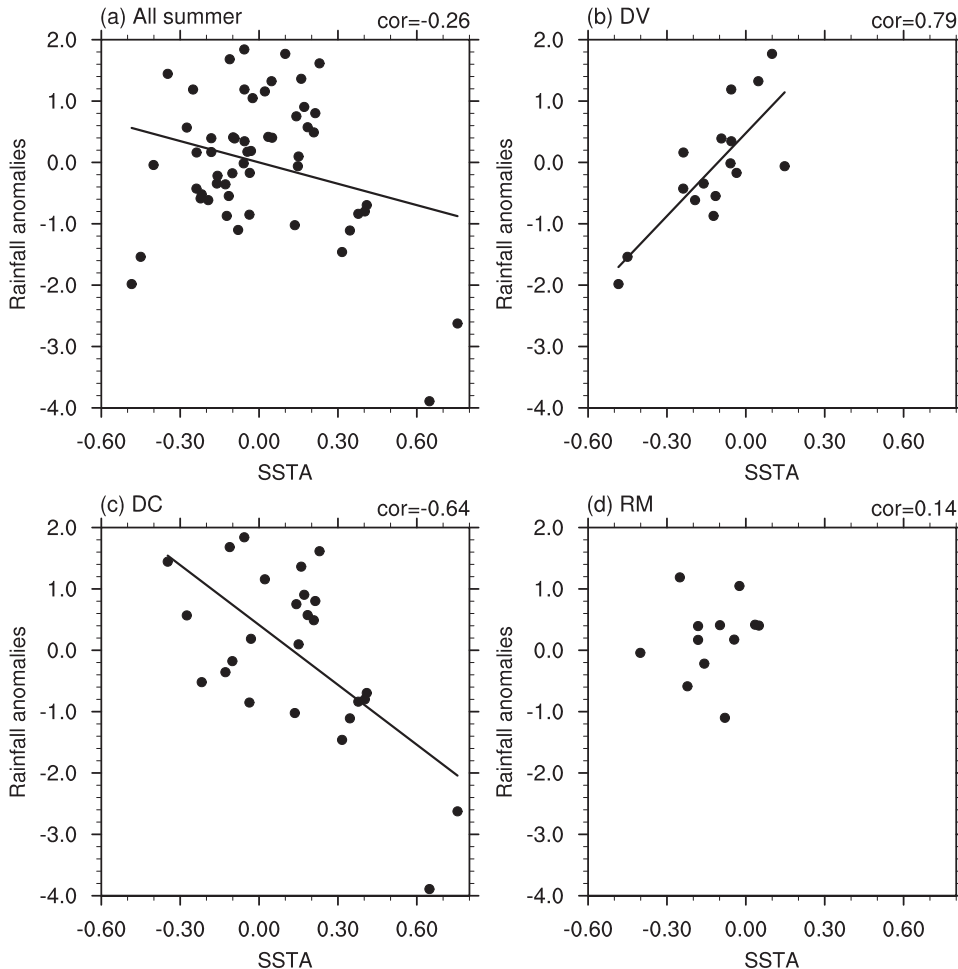


FIG. 2. Scatter diagrams of the area-averaged ( $2.5^{\circ}$ – $15^{\circ}$ N,  $120^{\circ}$ – $140^{\circ}$ E) precipitation and SST anomalies for (a) all summers of 1979–2005, (b) ENSO-developing summers, (c) ENSO-decaying summers, and (d) remaining summers. Precipitation anomalies are derived from the CMAP dataset and GPCP dataset, respectively. SST anomalies are derived from the HadISST dataset and ERSST dataset, respectively. The area-averaged rainfall–SST correlation coefficients are written at the top-right corner of each panel.

The positive correlation in the DV type (Fig. 2b) largely counteracts the negative correlation in the DC type (Fig. 2c), and thus makes the negative correlation in all of the summers insignificant. We calculate the partial correlation between precipitation and SST in the WNP, with the effect of remote forcing from the equatorial central-eastern Pacific, which is represented by the Niño-3 index, removed. The partial correlation coefficient reaches 0.36, which is larger than the original correlation coefficient 0.26, and exceeds 5% significance level.

To understand the cause of the reversed rainfall–SST relationships between ENSO-developing and ENSO-decaying summers, note the composite rainfall, SST patterns, and 850-hPa wind as shown in Fig. 3. The composite fields at the 10% local significance level are shaded. Based on the 10% local significance level, we test the field significance of the composite fields over the

WNP ( $0^{\circ}$ – $25^{\circ}$ N,  $110^{\circ}$ – $160^{\circ}$ E), by using Monte Carlo simulation (Livezey and Chen 1983). The experiments were completed 1000 times for each field test. The composite precipitation both in the DV type and in the DC type exceeds the 5% significance level. The composite SST in the DV (DC) type exceeds the 10% (15%) significance level. The composite zonal wind both in the DV type and in the DC type exceeds the 5% significance level.

For the DV type, the most pronounced SST signal is the warm SSTA in the equatorial central-eastern Pacific. Negative SST anomalies appear in the WNP, the Maritime Continent, and the southeastern Indian Ocean (IO; Fig. 3a). A reversed Walker circulation appears in the equatorial Pacific, with anomalous ascending (descending) motion in the central equatorial Pacific (Maritime Continent). Thus, the negative rainfall anomaly in the western Pacific is to a large extent a direct response to

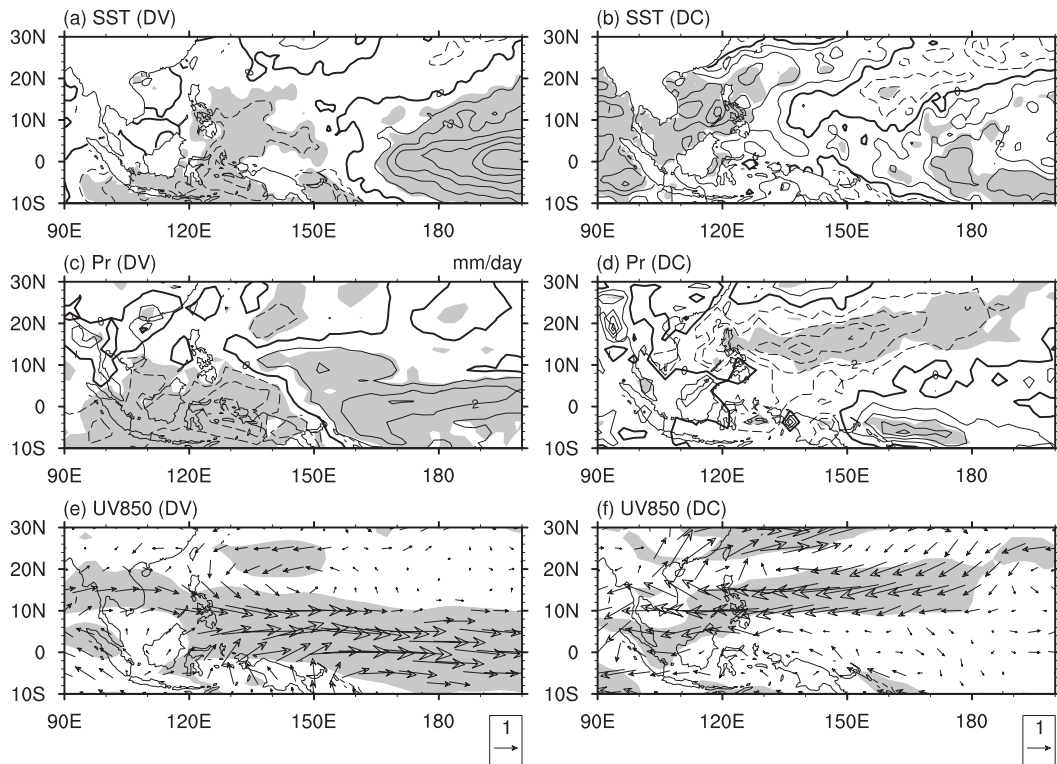


FIG. 3. Composite patterns of (a) SSTA ( $^{\circ}\text{C}$ ), (c) precipitation anomalies ( $\text{mm day}^{-1}$ ), and (e) 850-hPa wind anomalies ( $\text{m s}^{-1}$ ) for ENSO-developing summers. (b),(d),(f) Same as (a),(c), and (e), but for ENSO-decaying summers. Solid (dashed) lines represent positive (negative) values. The contour intervals of (a),(b) and (c),(d) are 0.15 and 1, respectively. Shading represents the 10% significance level.

the central Pacific heating associated with El Niño. The subsidence would reduce the cloud amount and cause the warm SSTA in the western Pacific. However, this cloud shortwave radiation effect is offset by the surface latent heat flux anomaly associated with the change of wind speed, as discussed below.

The maximum precipitation anomalies are primarily located in the equatorial central Pacific and over the WNP around  $5^{\circ}$ – $15^{\circ}\text{N}$ ,  $140^{\circ}$ – $160^{\circ}\text{E}$ . The former is a direct response to the El Niño warming, which is symmetric about the equator. In response to the symmetric heating, strong westerly anomalies at the equator and twin cyclones off the equator would be generated according to the classical Matsuno (1966)–Gill (1980) pattern. Because of the equatorial asymmetry of the summer mean flow (e.g., a strong easterly vertical shear over the WNP monsoon region), the anomalous cyclone is most pronounced in the WNP (Wang et al. 2003). The enhanced convection/rainfall anomalies north of the equator (around  $5^{\circ}$ – $15^{\circ}\text{N}$ ,  $140^{\circ}$ – $160^{\circ}\text{E}$ ) further induce antisymmetric circulation responses (Gill 1980). As seen from the anomalous wind field in Fig. 3b, northward cross-equatorial flows appear over the western Pacific and Maritime Continent regions from  $90^{\circ}$  to  $160^{\circ}\text{E}$ . This

WNP monsoon–southeastern (IO) teleconnection pattern may be referred to as the “Philippine–Sumatra pattern,” which has been noted previously in the study of the IO dipole (Li et al. 2002) and the origin of the tropospheric biennial oscillation (Li et al. 2006). Because the mean flow in boreal summer is the northward cross-equatorial flow, turning into the westerly flow under the WNP monsoon trough, the anomalous flows are approximately parallel to the mean flow in the region. The southeasterly anomaly off of Sumatra induces the cold SSTA through enhanced coastal upwelling, surface evaporation, and ocean vertical mixing (Li et al. 2003). The cold SSTA and associated suppressed convective anomaly south of the equator may further enhance the antisymmetric heating anomaly. As a result, the total surface wind speed over the Maritime Continent and the WNP monsoon trough region is greatly enhanced. The strengthened wind speed leads to the increase of surface latent heat flux, which overcomes the cloud shortwave radiation effect and causes the cold in situ SSTA. Thus, it is the combination of the overturning circulation associated with the remote El Niño forcing and the local latent heat flux effect associated with the variability of the WNP monsoon that leads to a positive

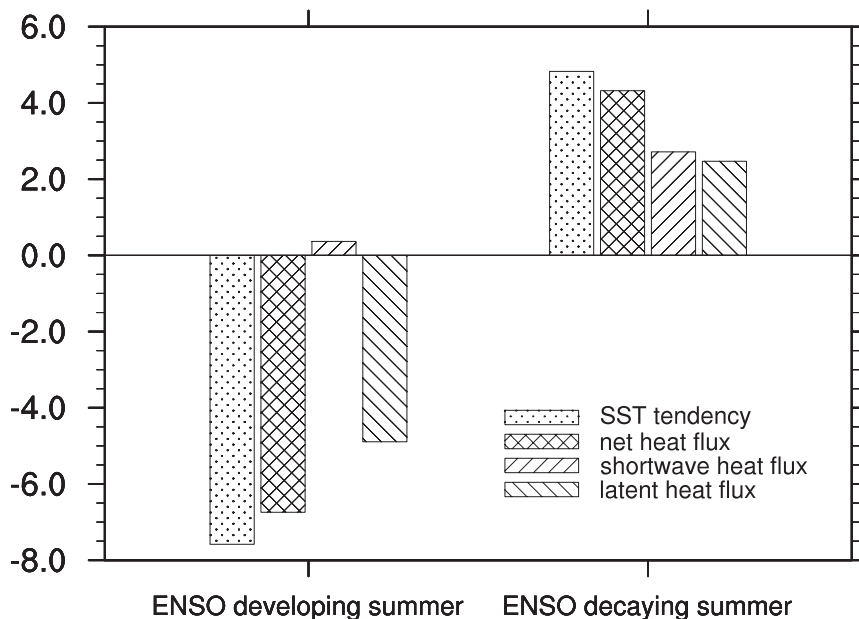


FIG. 4. The composite SSTA tendency, net downward heat flux anomalies, shortwave radiative flux anomalies, and latent heat flux anomalies averaged over  $0^{\circ}$ – $15^{\circ}$ N,  $120^{\circ}$ – $140^{\circ}$ E during the ENSO-developing and ENSO-decaying summers ( $\text{W m}^{-2}$ ). The SSTA tendency has been converted into the heat flux unit by assuming a constant ocean mixed layer depth of 80 m.

rainfall–SST relationship in the ENSO-developing summer.

For the DC type, the SSTA rapidly decays from its peak phase in the equatorial eastern-central Pacific, and by the summer, SST in the region is about normal (Fig. 3c). Positive SST anomalies occupy the WNP, South China Sea (SCS), and tropical IO. The most prominent feature of precipitation is a negative center extending from the SCS to the central North Pacific. This negative rainfall anomaly pattern is closely related to an anomalous anticyclone at 850 hPa in the region. The cause of this anomalous anticyclone has been discussed in previous studies (Chen et al. 2007; Wang et al. 2000; Wang and Zhang 2002). It develops in winter during the El Niño peak phase, and it is maintained to the subsequent spring and summer through either a local wind evaporation–SST feedback (Wang et al. 2000, 2003) or a remote forcing from the tropical IO (Yang et al. 2007).

The anomalous easterly to the south of the Philippine Sea anticyclone reduces the mean monsoon westerly and thus decreases the total surface wind speed. The accordingly reduced surface latent heat flux, together with the increased shortwave radiation resulting from the cloud reduction, leads to a warm SSTA in the western Pacific. As a result, the rainfall and SST anomalies have a remarkable negative correlation in the WNP during the

ENSO-decaying summer. It follows that the maintenance of the Philippine Sea anticyclone (cyclone) after the peak phase of El Niño (La Niña) dominates the generation of the negative SST–rainfall relationship.

To examine the relative role of the surface latent heat flux and shortwave radiative flux anomalies in changing the local SST, in Fig. 4 we show the amplitudes of the SSTA tendency, the net surface heat flux anomaly (which consists of shortwave radiation, longwave radiation, latent heat flux, and sensible heat flux components), and the surface latent and shortwave radiative flux anomalies in the region. The SST tendency is calculated using one order central difference scheme on each month. The JJA mean SST tendency and heat fluxes are calculated and shown in Fig. 4. Because the mean thermocline is deep in the WNP warm pool, the effect of the thermocline variation on the SSTA is relatively weak. The surface latent heat flux and shortwave radiative flux anomalies are the most dominant terms that change the local SST. To reduce uncertainties in the surface heat fluxes, an ensemble approach that averages the heat flux products from both the NCEP–NCAR reanalysis and OAF flux datasets is applied. For the DV type, the SSTA tendency and the total surface flux anomaly are consistently negative over the WNP region. On the contrary, for the DC type, the SST tendency and the total surface flux are consistently positive over the same region.

For the DV type, because the loss of the latent heat flux from the ocean is primarily attributed to the surface wind speed change, the spatial pattern of the latent heat flux anomaly generally resembles that of the surface wind speed anomaly (figure not shown). Compared to the latent heat flux, the positive shortwave radiative flux anomaly corresponding to the local suppressed convection is much smaller. Thus, the negative SSTA tendency is dominated by the negative latent heat flux anomaly associated with the enhanced cross-equatorial monsoonal flow. The SSTA cooling over the Maritime Continent is also primarily caused by the in situ negative latent heat flux anomaly.

For the DC type, both the latent heat flux and shortwave radiation flux anomalies contribute to the positive SST tendency (Fig. 4). Because the anomalous shortwave radiation is primarily determined by changes in the local cloud cover, the spatial pattern of the shortwave radiation flux anomaly is generally consistent with that of the suppressed convection over the WNP (figure not shown). Whereas the positive shortwave flux anomaly is associated with the suppressed convection, the positive latent heat flux anomaly is primarily attributed to the weakened surface wind speed. Both processes contribute to the negative SST–rainfall correlation during the ENSO-decaying summer.

Compared with the DV summer, the latent heat flux in DC summer plays a minor role in the SST tendency. It may be caused by the northward shift of anticyclonic anomalies in the DC type relative to cyclonic anomalies in the DV type. The mean state southwesterly wind of the WNP summer monsoon is located in the band of  $0^{\circ}$ – $10^{\circ}$ N. North of the band, the southwesterly wind changes to southerly wind (figure not shown). Because zonal wind prevails in the southern flank of the anticyclone or cyclone, wind speed anomalies would be stronger when the mean wind has a strong zonal component. Therefore, latent heat flux anomalies in the target region in the DV type tend to be stronger than that in the DC type.

#### 4. Conclusions and discussion

In contrast to the previous finding of the negative summer rainfall–SST relationship over the WNP, we find that this relationship experiences a significant interannual variation. Separating the ENSO-developing (DV) and ENSO-decaying (DC) summers, we notice that for the DV type, the rainfall anomalies are significantly positively correlated with the SSTA over the WNP, whereas for the DC type, rainfall anomalies are significantly negatively correlated with SSTA. Thus, the overall negative rainfall–SST correlation is mainly contributed by the negative correlation in the ENSO-decaying sum-

mers. For the rest of summers there is no significant negative or positive rainfall–SST correlation over the WNP.

The significant positive rainfall–SST correlation in the DV type is attributed to the interplay between the anomalous Walker circulation and cross-equatorial flows associated with the Philippine–Sumatra pattern. The former, as a direct response to El Niño heating, leads to negative rainfall anomalies in the western Pacific; the latter leads to a cold SSTA resulting from enhanced WNP monsoon flows and surface latent heat fluxes. Because the latent flux anomaly dominates the total surface flux terms, it plays a fundamental role in generating the cold SSTA over the WNP and Maritime Continent region.

The negative rainfall–SST correlation in the DC type is primarily attributed to the formation of the anomalous Philippine Sea anticyclone that persists from the El Niño peak phase (boreal winter) to the subsequent summer. The anomalous anticyclone, on one hand, induces negative in situ rainfall anomalies, and on the other hand decreases the surface wind speed. Both the increase of downward shortwave radiation resulting from the suppressed convection and the decrease of upward latent heat fluxes resulting from the reduced wind speed contribute to a warming tendency in the WNP, leading to a negative rainfall–SST relationship.

In the DV summer, the negative SSTA in the WNP primarily results from the atmospheric forcing through latent heat flux. Meanwhile, the precipitation anomalies over the WNP are dominated by the large-scale Walker circulation. However, after the formation of the negative SSTA, it would increase the zonal anomalous temperature gradient, enhance the anomalous Walker circulation, and further suppress the local precipitation. The relative contribution of the SSTA to in situ precipitation anomalies needs further analysis.

In this work, we note the mechanisms responsible for the formation of negative SSTA in the WNP in the El Niño–developing summer. In fact, the negative SSTA persisted until the following summer (the El Niño–decaying summer; see Fig. 2c of Lau and Nath 2006). The maintenance of the negative SSTA after the ENSO mature phase is attributed to its coupling with the Philippine Sea anticyclone through positive wind–evaporation–SST feedback (Wang et al. 2000; Lau and Nath 2000). However, in the El Niño–decaying summer, with the onset of WNP summer monsoon, the positive feedback changes to a negative feedback, and the negative SSTA gradually evolves to positive (Wu et al. 2009). In terms of our analysis, both the latent heat flux and shortwave radiation are responsible for the SST warming, but their relative contribution need further numerical study because of the limitation of the observational flux data.

**Acknowledgments.** This work was supported by NSFC Grants 40628006, 40523001, and 40821092; the National Basic Research Program of China (2006CB403603); and the China Meteorological Administration under Grants GYHY20070610 and GYHY200706005. TL was also supported by ONR Grants N000140710145, N00173061G031, and N000140810256, and by the International Pacific Research Center, which is sponsored by the Japan Agency for Marine–Earth Science and Technology (JAMSTEC), NASA (NNX07AG53G), and NOAA (NA17RJ1230).

## REFERENCES

- Adler, R. F., and Coauthors, 2003: The Version 2 Global Precipitation Climatology Project (GPCP) Monthly Precipitation Analysis (1979–present). *J. Hydrometeorol.*, **4**, 1147–1167.
- Chen, J. M., T. Li, and C. F. Shih, 2007: Fall persistence barrier of sea surface temperature in the South China Sea associated with ENSO. *J. Climate*, **20**, 158–172.
- Gill, A. E., 1980: Some simple solutions for heat-induced tropical circulation. *Quart. J. Roy. Meteor. Soc.*, **106**, 447–462.
- Kalnay, E., and Coauthors, 1996: The NCEP/NCAR 40-Year Reanalysis Project. *Bull. Amer. Meteor. Soc.*, **77**, 437–471.
- Kumar, A., and M. P. Hoerling, 2003: The nature and causes for the delayed atmospheric response to El Niño. *J. Climate*, **16**, 1391–1403.
- Lau, N. C., and M. J. Nath, 2000: Impact of ENSO on the variability of the Asian–Australian monsoons as simulated in GCM experiments. *J. Climate*, **13**, 4287–4309.
- , and —, 2006: ENSO modulation of the interannual and intraseasonal variability of the East Asian monsoon—A model study. *J. Climate*, **19**, 4508–4530.
- Li, T., Y. S. Zhang, E. Lu, and D. L. Wang, 2002: Relative role of dynamic and thermodynamic processes in the development of the Indian Ocean dipole: An OGCM diagnosis. *Geophys. Res. Lett.*, **29**, 2110, doi:10.1029/2002GL015789.
- , B. Wang, C. P. Chang, and Y. S. Zhang, 2003: A theory for the Indian Ocean dipole–zonal mode. *J. Atmos. Sci.*, **60**, 2119–2135.
- , P. Liu, X. Fu, B. Wang, and G. A. Meehl, 2006: Spatiotemporal structures and mechanisms of the tropospheric biennial oscillation in the Indo-Pacific warm ocean regions. *J. Climate*, **19**, 3070–3087.
- Livezey, R. E., and W. Y. Chen, 1983: Statistical field significance and its determination by Monte Carlo techniques. *Mon. Wea. Rev.*, **111**, 46–59.
- Matsuno, T., 1966: Quasi-geostrophic motions in the equatorial area. *J. Meteor. Soc. Japan*, **44**, 25–42.
- Rayner, N. A., D. E. Parker, E. B. Horton, C. K. Folland, L. V. Alexander, D. P. Rowell, E. C. Kent, and A. Kaplan, 2003: Global analyses of sea surface temperature, sea ice, and night marine air temperature since the late nineteenth century. *J. Geophys. Res.*, **108**, 4407, doi:10.1029/2002JD002670.
- Smith, T. M., R. W. Reynolds, T. C. Peterson, and J. Lawrimore, 2008: Improvements to NOAA’s historical merged land–ocean surface temperature analysis (1880–2006). *J. Climate*, **21**, 2283–2296.
- Trenberth, K. E., and D. J. Shea, 2005: Relationships between precipitation and surface temperature. *Geophys. Res. Lett.*, **32**, L14703, doi:10.1029/2005GL022760.
- Wang, B., and Q. Zhang, 2002: Pacific–East Asian teleconnection. Part II: How the Philippine Sea anomalous anticyclone is established during El Niño development. *J. Climate*, **15**, 3252–3265.
- , R. G. Wu, and X. H. Fu, 2000: Pacific–East Asian teleconnection: How does ENSO affect East Asian climate? *J. Climate*, **13**, 1517–1536.
- , —, and T. Li, 2003: Atmosphere–warm ocean interaction and its impacts on Asian–Australian monsoon variation. *J. Climate*, **16**, 1195–1211.
- , I. S. Kang, and J. Y. Lee, 2004: Ensemble simulations of Asian–Australian monsoon variability by 11 AGCMs. *J. Climate*, **17**, 803–818.
- , Q. Ding, X. Fu, I.-S. Kang, K. Jin, J. Shukla, and F. Doblas-Reyes, 2005: Fundamental challenge in simulation and prediction of summer monsoon rainfall. *Geophys. Res. Lett.*, **32**, L15711, doi:10.1029/2005GL022734.
- Wu, B., T. J. Zhou, and T. Li, 2009: Seasonally evolving dominant interannual variability modes of East Asian Climate. *J. Climate*, **22**, 2992–3005.
- Wu, R. G., and B. P. Kirtman, 2007: Regimes of seasonal air–sea interaction and implications for performance of forced simulations. *Climate Dyn.*, **29**, 393–410.
- , —, and K. Pegion, 2006: Local air–sea relationship in observations and model simulations. *J. Climate*, **19**, 4914–4932.
- Xie, P., and P. A. Arkin, 1997: Global precipitation: A 17-year monthly analysis based on gauge observation, satellite estimate, and numerical model outputs. *Bull. Amer. Meteor. Soc.*, **78**, 2539–2558.
- Yang, J., Q. Liu, S.-P. Xie, Z. Liu, and L. Wu, 2007: Impact of the Indian Ocean SST basin mode on the Asian summer monsoon. *Geophys. Res. Lett.*, **34**, L02708, doi:10.1029/2006GL028571.
- Yu, L., X. Jin, and R. A. Weller, 2008: Multidecade Global Flux Datasets from the Objectively Analyzed Air–sea Fluxes (OAF–lux) Project: Latent and sensible heat fluxes, ocean evaporation, and related surface meteorological variables. Woods Hole Oceanographic Institution, OAFlux Project Tech. Rep. OA-2008-01, 64 pp.
- Zhou, T., R. Yu, H. Li, and B. Wang, 2008a: Ocean forcing to changes in global monsoon precipitation over the recent half-century. *J. Climate*, **21**, 3833–3852.
- , and Coauthors, 2008b: The CLIVAR C20C Project: Which components of the Asian–Australian Monsoon circulation variations are forced and reproducible? *Climate Dyn.*, doi:10.1007/s00382-008-0501-8, in press.
- , B. Wu, and B. Wang, 2009: How well do atmospheric general circulation models capture the leading modes of the interannual variability of the Asian–Australian monsoon? *J. Climate*, **22**, 1159–1173.